Pei Feng[1,2],
Dashuang Liu[1],
Ronggen Zhang[1],
Chongchang Yang[1,2]*

Distribution of the Polymer Melt Velocity and Temperature in the Spinneret Channel of Bi-component Fibre Melt Spinning: a Mathematical Model

DOI: 10.5604/01.3001.0015.2722

[1] Donghua University,
College of Mechanical Engineering,
Shanghai, 201620, China

[2] Engineering Research Center
of Advanced Textile Machinery,
Ministry of Education,
Shanghai, 201620, China,
* e-mail: pfeng@dhu.edu.cn

Abstract
For the stability of composite fibre spinning, the difference in and distribution of the polymer melt velocity during the spinning are among the factors of importance. Based on the basic equation for the control of composite spinning dynamics, boundary conditions are identified and reported in this paper. A mathematical model for the symmetric and asymmetric distribution of the melt flow velocity in the microhole of the spinneret of the composite spinning assembly was developed. The accuracy of the mathematical model was also ascertained. It gives a theoretical basis for the designing of a composite spinning assembly.

Key words: *composite fibre, spinning assembly, velocity field distribution, mathematical model.*

Introduction

With the emergence of the demand for smart, functional and other new types of fibres, traditional fibre materials are being endowed with electrical, optical, information transmission, storage and other functions [1]. Composite fibre is the main variety of functional fibre, used in industries dedicated to the military, hospitals and high-end special fields like anti-counterfeiting, anti-statics, shielding etc.

To prepare composite fibre, two or more polymer melts or solutions with different properties are taken, and use of the ratio and viscosity of components is made to introduce difference in the variety. The melts or solutions are made to flow into the spinning equipment, merged in a certain part, and squirted out from the same spinneret micropore to form a fibre [2-3]. Fibre composite types include the juxtaposition composite, leather core composite, peel composite, etc., shown in ***Figure 1***. Currently, research on new composite fibres is mainly focused on the leather core composite and parallel composite [4-6].

Literature reports [7-8] on research on the theory of composite fibre spinning are focused on the influence of different structural and technological parameters on crimp ability. Research groups [9-11] carried out a spinning simulation of the dynamics of composite spinning with a leather core and developed a mathematical model of the temperature and heat conduction of a fibre section.

To design composite fibre spinning components, the difference in the flow velocity and field distribution between the two polymers in the orifice are the key parameters. However, at present, the design of spinning components and the determination of process parameters depend mainly on tradition and experience, and mathematical models of the temperature and velocity field distribution of composite melt flow, for theoretical guidance, have not been developed. Therefore, boundary conditions were identified for different orifice conditions, and a mathematical model for the melt velocity and temperature field distribution of two kinds of polymers in the orifice of a composite spinning spinneret was developed in this paper.

Mathematical modeling

The melt wall slip is presumed, and the slip velocity at the wall is *Vs*, and *Vs* is 0 when there is no slip. The cross section of composite fibre is divided into symmetric and asymmetric shapes. The boundary conditions are described according channel shapes, and the mathematical model for the velocity field distribution is derived. In order to simplify the calculation, the extrusion flow process of the composite fibre polymer melt is assumed as follows without involving crystallisation and orientation.

(1) The polymer melt is incompressible.

(2) The polymer melt flow is stable and laminar.

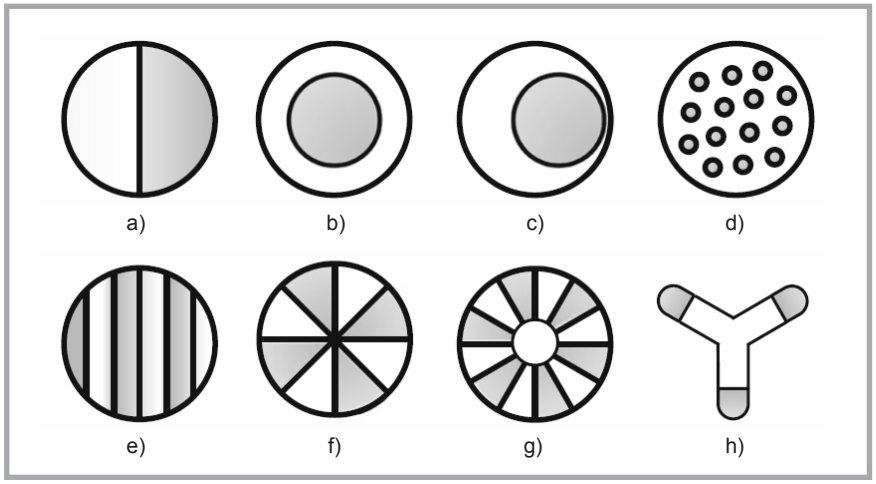

Figure 1. *Variety of bi-component fibre cross-sections: a) side-by-side, sheath-core with concentric b) and eccentric c) configurations, d) islands-in-the-sea, e) alternating segments with stripes, f) pies, g) citrus, h) tipped trilobal [3].*

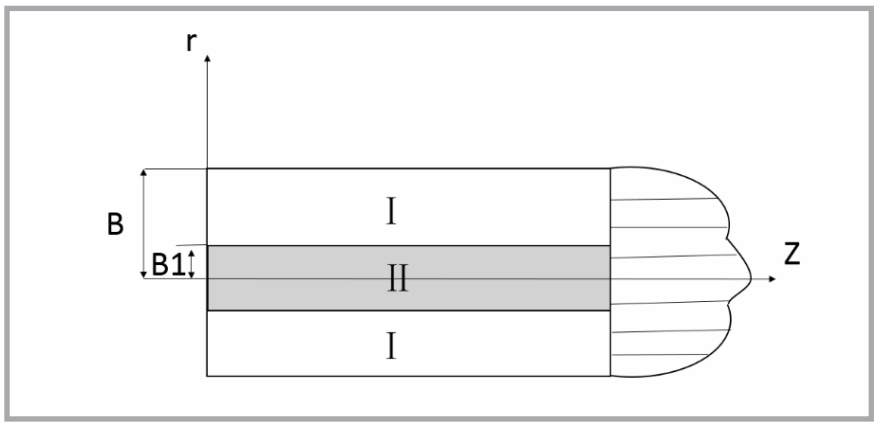

Figure 2. *Schematic diagram of the symmetrically distributed flow model of the composite melt.*

(3) The temperature of the polymer melt does not change with time, and the thermal convection is negligible. It is presumed that the heat conduction and viscosity dissipation dominate the temperature field and that the temperature of channel walls remains unchanged.

(4) The difference in density between the two melts has no influence on the flow.

(5) The relationship between the flow dynamics and heat of the two polymer melts is ignored.

(6) The change in viscosity of the polymer melt is related to the temperature, and follows the Arrhenius relationship.

For melt spinning, the basic equations used in general simulation research are shown in ***Table 1***.

Velocity field distribution

The fibre cross-section shapes are considered symmetrical and asymmetrical separately. Therefore, two kinds of polymers are considered in the flow through the channel resulting in composite profiled fibre. The melt is assumed as wall slippage, and the wall slip velocity according to the channel condition controls the boundary conditions. The velocity field and temperature field distribution function are derived theoretically.

Symmetric distribution

The hole is assumed as being symmetric in shape, similar to that of a sheath-core composite fibre. The core layer of the melt is considered as a completely covered cortex melt. The polymer melt flow is assumed as the total flow exhibited. The direction of shear velocity is parallel to the axis, similar to one-dimensional laminar flow, at constant pressure gradient on the cross section. The time has no effect on the flow and maximum speed occurring in melt II. Thus, there are two kinds of polymer melt flow, as shown in ***Figure 2***.

The boundary conditions are as follows:

a. when r = 0, shear stress $\tau = 0$, $\frac{\partial T}{\partial r} = 0$, $\frac{\partial T}{\partial r} = 0$;

Table 1. *Governing equation of melt spinning dynamics.*

Energy balance equation	$\frac{dT}{dx} = -\frac{2\sqrt{\pi A}h}{GC_p}(T - T_s)$
Conservation of mass equation	$W = A(x)\rho(T)V(x) = \frac{\rho(T)V(x)\pi d^2(x)}{4}$
Momentum conservation equation	$\frac{dF}{dx} = W\left(\frac{dV}{dx}\right) + 2\pi RP_{xr} - \pi\sigma\left(\frac{dR}{dx}\right) - \pi\rho gR^2$
Constitutive equation	$\frac{dV(x)}{dx} = \frac{F(x)}{A\eta_e}$

b. when r = B_1, the velocities on both sides of the interface are equal $v_{z1} = v_{z2}$, $\tau_{rz1} = \tau_{rz2}$, $T_1 = T_2$;

c. when r = B, there is slip on the wall surface and the velocity is v_s, then $v_{z1} = v_s$, $T_1 = T_w$.

The z-component of the momentum conservation equation in the cylindrical coordinate system is:

$$\frac{\partial F/A}{\partial z} = \frac{1}{r}\frac{\partial(r\cdot\tau_{rz})}{\partial r} + \frac{1}{r}\frac{\partial(\tau_{\theta z})}{\partial\theta} + \frac{\partial(\tau_{zz})}{\partial z} \tag{1}$$

Since the flow is a one-dimensional laminar, the derivative of z with respect to z and the z-direction component of shear stress is 0. ***Equation (1)*** becomes:

$$\frac{\partial F/A}{\partial z} = \frac{1}{r}\frac{\partial(r\tau_{rz})}{\partial r} \tag{2}$$

On integrating both sides:

$$\tau_{rz} = \frac{1}{2}\left(\frac{dF/A}{dz}\right)r + \frac{C_1}{r} \tag{3}$$

and using $\zeta = -\frac{dF}{dz}$, the shear stress equation becomes:

$$\tau_{rz} = -\frac{1}{2}\zeta r + \frac{C_1}{r} \tag{4}$$

The integral constant obtained from the boundary conditions rearranges the shear stress equation as:

$$\tau_{rz} = -\frac{1}{2}\zeta r \tag{5}$$

The constitutive equations for the power law of the fluid are:

$$\tau_{rz} = K_1\cdot\dot{\gamma}^n = K_1\left(\frac{dv_{z_1}}{dr}\right)^{n_1} \tag{6}$$

$$\tau_{rz} = K_2\cdot\dot{\gamma}^n = K_2\left(\frac{dv_{z_2}}{dr}\right)^{n_2} \tag{7}$$

Where, K is the melt consistency, γ the shear rate, and n the non-Newtonian exponent.

On integrating ***Equations (6)*** and ***(7)***, and after simplification the velocity distribution functions of the composite profiled spinning are:

Melt I:

$$v_{z1} = v_s + \frac{n_1}{n_1+1}\left(\frac{\zeta}{2K_1}\right)^{\frac{1}{n_1}}\cdot\left(B^{\frac{n_1+1}{n_1}} - r^{\frac{n_1+1}{n_1}}\right) \tag{8}$$

Melt II:

$$v_{z2} = \frac{n_1}{n_1+1}\left(\frac{\zeta}{2K_1}\right)^{\frac{1}{n_1}}\cdot\left(B^{\frac{n_1+1}{n_1}} - B_1^{\frac{n_1+1}{n_1}}\right) + \frac{n_2}{n_2+1}\left(\frac{\zeta}{2K_2}\right)^{\frac{1}{n_2}}\cdot\left(B^{\frac{n_2+1}{n_2}} - r^{\frac{n_2+1}{n_2}}\right) \tag{9}$$

Asymmetric distribution

The two polymers melts flow next to each other and the channel shape is asymmetric. The two polymer components are in contact with the surface of the wall, and the boundary layer is common. Due to the differences in the properties of melts, the distribution of the velocity field is discontinuous, a model diagram of the flow is shown in ***Figure 3***.

For the two kinds of melts, the viscosities are different, and therefore the maximum speed is located on the low viscosity side. Assuming that for melt II the viscosity is higher than that of I, the maximum speed occurs as shown ***in Figure 3***. Boundary conditions are as follows:

(1) when r = B_0, the speed is largest $v = v_{max}$, and shear stress $\tau_{rz2} = 0$;
(2) when r = B_1, the velocities on both sides of the interface are equal, $v_{z1} = v_{z2}$, $\tau_{rz1} = \tau_{rz2}$;
(3) when r = B, the velocity of the wall is v_{s1}, $v_{z1} = v_{s1}$, $T_1 = T_w$;
(4) when r = 0, the velocity of the wall is v_{s2}, $v_{z2} = v_{s2}$.

When $0 \le r \le B_0$, the velocity gradient is positive and $\frac{dv_z}{dr} > 0$.

The z-component of the momentum conservation ***Equation (1)*** in the cylindrical coordinate system is:

$$\frac{\partial F/A}{\partial z} = \frac{1}{r}\frac{\partial(r\tau_{rz})}{\partial r} + \frac{1}{r}\frac{\partial(\tau_{\theta z})}{\partial \theta} + \frac{\partial(\tau_{zz})}{\partial z} \tag{10}$$

Using the assumptions and boundary conditions, ***Equation (10)*** is simplified as:

$$\frac{\partial F/A}{\partial z} = \frac{1}{r}\frac{\partial(r\tau_{rz})}{\partial r} \tag{11}$$

Its integration gives (12):

$$\tau_{rz} = \frac{1}{2}(\frac{dF}{dz})r + \frac{C}{r} \tag{12}$$

Using $\zeta = \frac{dF}{dz}$, the expression of shear stress is obtained as: $\tau_{rz} = \frac{1}{2}\zeta r + \frac{C}{r}$.

By applying the boundary condition r = B_0 to the equation above, the integral constant is obtained, and the equation is reduced to:

$$\tau_{rz} = \frac{\zeta}{2}(\frac{r^2 - B_0^{\,2}}{r}) \tag{13}$$

Equation (13) can be obtained also by integrating the constitutive equation of the power-law of fluid and ***Equation (12)***.

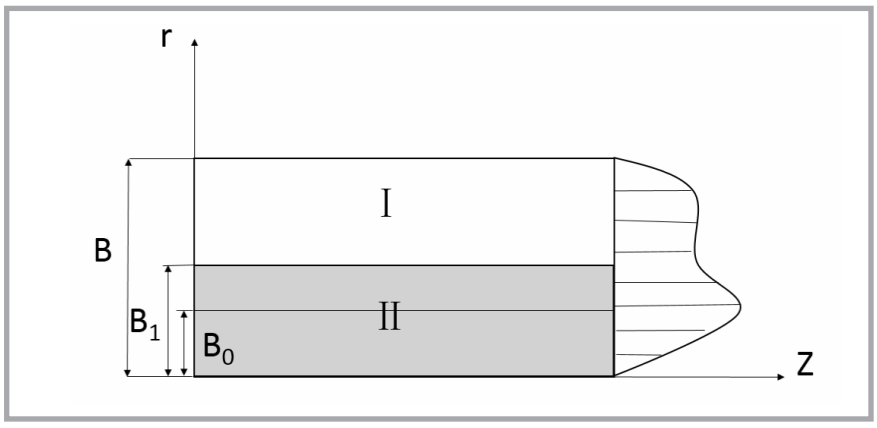

Figure 3. *Schematic diagram of the asymmetric distribution model of the composite flow.*

Melt II:

$$\int_0^r v_{z2} = v_{z2}(r) - v_{z2}(r=0) =$$
$$= (\frac{\zeta}{2K_2})^{\frac{1}{n_2}} \int_0^r (\frac{r^2 - B_0^{\,2}}{r})^{\frac{1}{n_2}} dr \tag{14}$$

On using the boundary conditions of $r = 0$, the velocity distribution of melt II can be obtained as:

$$v_{z2} = v_{s2} + (\frac{\zeta}{2K_2})^{\frac{1}{n_2}} \int_0^r (\frac{r^2 - B_0^{\,2}}{r})^{\frac{1}{n_2}} dr \tag{15}$$

When $B_0 \le r \le B$, the velocity gradient is negative. Then $\frac{dv_z}{dr} < 0$. Since there are two kinds of polymer melts, the integration of both results in the velocity distribution function of the two, respectively.
For melt I:

$$\int_r^B v_{z1} = v_{s1} + v_{z1}(r=B) - v_{z1}(r) =$$
$$= (\frac{\zeta}{2K_1})^{\frac{1}{n_1}} \int_r^R (\frac{r^2 - B_0^{\,2}}{r})^{\frac{1}{n_1}} dr \tag{16}$$

On applying boundary conditions: $r = B$, the melt I velocity distribution function is obtained as:

$$v_{z1} = v_{s1} + (\frac{\zeta}{2K_1})^{\frac{1}{n_1}} \int_r^B (\frac{B_0^{\,2} - r^2}{r})^{\frac{1}{n_1}} dr$$
$$(B_1 \le r \le B) \tag{17}$$

For melt II:

$$\int_r^{B_1} v_{z2} = v_{z2}(r=B_1) - v_{z2}(r) =$$
$$= (\frac{\zeta}{2K_2})^{\frac{1}{n_2}} \int_r^{B_1} (\frac{r^2 - B_0^{\,2}}{r})^{\frac{1}{n_2}} dr \tag{18}$$

Simplification of the above equation gives:

$$v_{z2} = (\frac{\zeta}{2K_2})^{\frac{1}{n_2}} \int_r^{B_1} (\frac{B_0^{\,2} - r^2}{r})^{\frac{1}{n_2}} dr +$$
$$+ v_{z2}(r=B_1) \quad (B_1 \le r \le B) \tag{19}$$

When $r = B_0$, the velocity values in ***Equations (17)*** and ***(19)*** become the same. Thus

$$(\frac{\zeta}{2K_2})^{\frac{1}{n_2}} \int_0^{B_0} (\frac{r^2 - B_0^{\,2}}{r})^{\frac{1}{n_2}} dr =$$
$$= (\frac{\zeta}{2K_2})^{\frac{1}{n_2}} \int_{B_0}^{B_1} (\frac{B_0^{\,2} - r^2}{r})^{\frac{1}{n_2}} dr + v_{z2}(r=B_1) \tag{20}$$

According to ***Equation (20)***:

$$v_{z2}(r=B_1) = (\frac{\zeta}{2K_2})^{\frac{1}{n_2}} [\int_0^{B_0} (\frac{r^2 - B_0^{\,2}}{r})^{\frac{1}{n_2}} dr -$$
$$+ \int_{B_0}^{B_1} (\frac{B_0^{\,2} - r^2}{r})^{\frac{1}{n_2}} dr] \tag{21}$$

On combining ***Equations (21)*** with ***(19)***, the velocity distribution of melt II can be obtained.

In summary, the velocity distributions of the two polymer melts are;

For melt I,

$$v_{z1} = v_{s1} + (\frac{\zeta}{2K_1})^{\frac{1}{n_1}} \int_r^B (\frac{B_0^{\,2} - r^2}{r})^{\frac{1}{n_1}} dr$$
$$(B_1 \le r \le B) \tag{22}$$

For melt II,

$$v_{z2} = (\frac{\zeta}{2K_2})^{\frac{1}{n_2}} \int_r^{B_1} (\frac{B_0^{\,2} - r^2}{r})^{\frac{1}{n_2}} dr +$$
$$+ (\frac{\zeta}{2K_2})^{\frac{1}{n_2}} [\int_0^{B_0} (\frac{r^2 - B_0^{\,2}}{r})^{\frac{1}{n_2}} dr -$$
$$+ \int_{B_0}^{B_1} (\frac{B_0^{\,2} - r^2}{r})^{\frac{1}{n_2}} dr] \quad (B_0 \le r \le B_1) \tag{23}$$

$$v_{z2} = v_{s2} + (\frac{\zeta}{2K_2})^{\frac{1}{n_2}} \int_0^r (\frac{r^2 - B_0^{\,2}}{r})^{\frac{1}{n_2}} dr$$
$$(0 \le r \le B_0) \tag{24}$$

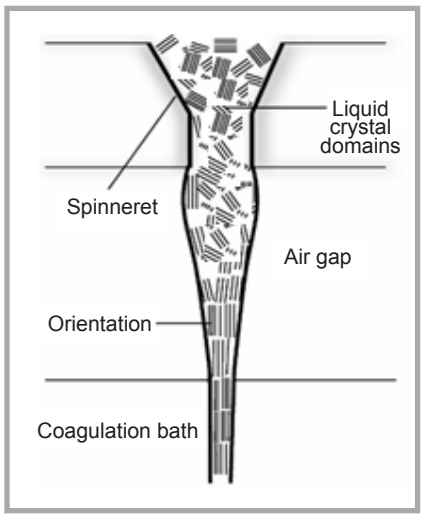

Figure 4. *Geometric model of parallel compound extrusion.*

Temperature field distribution

Similar to the flow distribution model for the velocity field of the composite, the temperature field distribution can be divided into two types, viz symmetric and asymmetric.

Symmetric distribution

According to the Fourier law of heat conduction, the heat flux q is:

$$q = -K_c \nabla T \tag{25}$$

Substitution of the constitutive equation of the power-law of fluid into the energy balance equation in ***Table 2*** results in:

$$K_1\left(\frac{\partial v_{z1}}{\partial r}\right)^{n_1+1} = K_1 \dot{\gamma}^{n_1+1} = \tau_{rz1}\frac{\partial v_{z1}}{\partial r} = -\frac{K_{c1}}{r}\frac{\partial}{\partial r}\left(r\frac{\partial T_1}{\partial r}\right) \tag{26}$$

$$K_2\left(\frac{\partial v_{z2}}{\partial r}\right)^{n_2+1} = K_2 \dot{\gamma}^{n_2+1} = \tau_{rz2}\frac{\partial v_{z2}}{\partial r} = -\frac{K_{c2}}{r}\frac{\partial}{\partial r}\left(r\frac{\partial T_2}{\partial r}\right) \tag{27}$$

Combining the constitutive equation of the power-law of fluid with the shear stress expression in ***Table 2*** results in:

$$\dot{\gamma}_1 = \left(\frac{r\zeta}{2K_1}\right)^{\frac{1}{n_1}} \tag{28}$$

$$\dot{\gamma}_2 = \left(\frac{r\zeta}{2K_2}\right)^{\frac{1}{n_2}} \tag{29}$$

Using ***Equations (26)***, ***(27)***, ***(28)*** and ***(29)***, with simplification and integration, the temperature distribution function can be obtained as:

Melt I:

$$r\left(\frac{\partial T_1}{\partial r}\right) = -\frac{K_1}{k_{c1}}\left(\frac{3n_1+1}{n_1}\right)\left(\frac{\zeta}{2K_1}\right)^{\frac{n_1+1}{n_1}} + C_2 = T_1 \tag{30}$$

Melt II:

$$r\left(\frac{\partial T_2}{\partial r}\right) = -\frac{K_2}{k_{c2}}\left(\frac{3n_2+1}{n_2}\right)\left(\frac{\zeta}{2K_2}\right)^{\frac{n_2+1}{n_2}} + C_3 = T_2 \tag{31}$$

C_2 and C_3, determined by the boundary conditions, give the following temperature distribution functions for two kinds of polymer melts with symmetric distribution:

$$T_1 - T_W = \frac{K_1}{k_{c1}}\left(\frac{n_1}{3n_1+1}\right)\left(\frac{\zeta}{2K_1}\right)^{\frac{n_1+1}{n_1}}\left(R^{\frac{3n_1+1}{n_1}} - r^{\frac{3n_1+1}{n_1}}\right) \tag{32}$$

$$T_{1(r=R_1)} = \frac{K_2}{k_{c2}}\left(\frac{n_2}{3n_2+1}\right)\left(\frac{\zeta}{2K_2}\right)^{\frac{n_2+1}{n_2}}\left(R^{\frac{3n_2+1}{n_2}} - R_1^{\frac{3n_2+1}{n_2}}\right) \tag{33}$$

Asymmetric distribution

When the flow of the two different polymer melts has an asymmetric distribution, the following formulae can be derived for the asymmetric temperature distribution:

$$-\frac{k_c B_0^{\,2}}{r}\cdot\frac{\partial}{\partial r}\left(r\frac{\partial T}{\partial r}\right) = K\dot{\gamma}^{n+1} \tag{34}$$

$$\tau_{rz} = \frac{B_0\zeta}{2}\left(\frac{B_0^{\,2}-r^2}{r^2}\right) \tag{35}$$

$$\tau_{rz} = K\dot{\gamma}^{n} \tag{36}$$

Based on the momentum conservation equation, power law equation and boundary conditions, the following equation results:

$$\dot{\gamma} = \left[\frac{B_0\zeta}{2K}\left(\frac{B_0^{\,2}-r^2}{r^2}\right)\right]^{\frac{1}{n}} \tag{37}$$

From ***Equations (34)***, ***(35)***, ***(36)*** & ***(37)***, and the boundary conditions, the temperature distribution function obtained after integration is:

Melt I:

$$T_1 = T_w + \left[\frac{K_1}{B_0^{\,2}k_{c1}}\left(\frac{B_0\zeta}{2K_1}\right)^{\frac{n_1+1}{n_1}}\right]\ln r \int_r^B r\left(\frac{B_0^{\,2}-r^2}{r^2}\right)^{\frac{n_1+1}{n_1}} dr \tag{38}$$

Melt II:

$$T_{1(r=B_1)} + \left[\frac{K_2}{B_0^{\,2}k_{c2}}\left(\frac{B_0\zeta}{2K_2}\right)^{\frac{n_2+1}{n_2}}\right]\left(\ln r - \ln B\right) \int_0^r r\left(\frac{B_0^{\,2}-r^2}{r^2}\right)^{\frac{n_2+1}{n_2}} dr \tag{39}$$

Simulation calculation

In order to verify the rationality and reliability of the above mathematical model of velocity field distribution, a melt with poor compatibility of the two kinds of polymer melts was used for verification. In this paper, the widely used polymer melts polyglycol terephthalate (PET) and polyamide (PA6) were used for juxtaposing to solve the velocity field distribution numerically. A geometric model was established, shown in ***Figure 4***.

In this paper, the velocity field distribution function is based on Euler's description method, which describes the velocity distribution point by point at any specified time and deduces the mathematical model by using the momentum equation. Based on the staggered grid finite volume method [11], the momentum equation was first discretised. According to the discretised momentum equation, the Fortran programming language was used to solve the velocity field distribution functions of two kinds of polymer melts combined with a simple algorithm. Specifically, S1 solves the momentum equation, and the velocity field under the specified viscosity field and temperature field are obtained. In S2 the viscosity field is resolved from the specified temperature field and known shear rate field. S3 repeats S1 and S2 until the velocity

Table 2. *Material parameters [11].*

Material parameters	PA6	PET
Nonnewtonian exponent n	0.75	0.66
Relaxation time λ, s^{-1}	0.02	0.07
Zero shear viscosity η_0, $(Pa{\cdot}s)^{-1}$	750	210
Density ρ, kg/m^3	973	1268

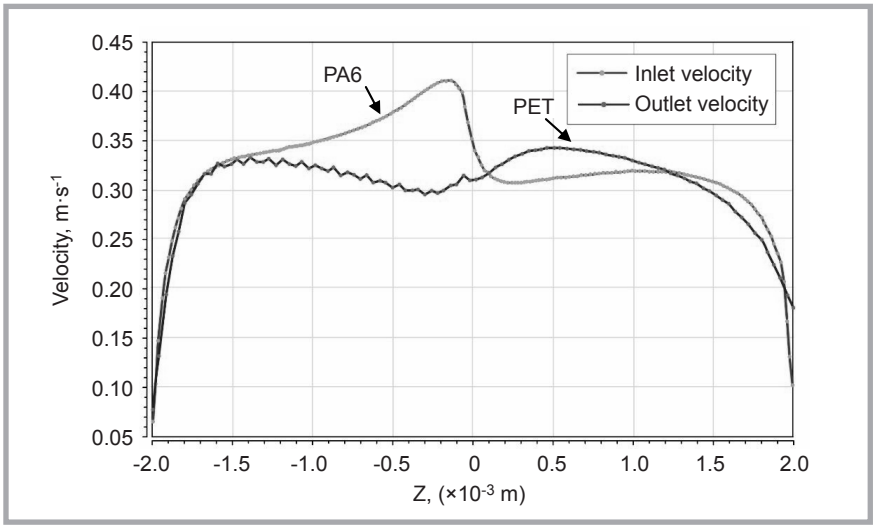

Figure 5. *Calculation results of the velocity field at the entrance and exit of PET and PA6 micropores.*

field, viscosity field and pressure field converge.

The convergence criterion is:

$$\left|\frac{\sum\left(u_i{}^{n'+1}-u_i{}^{n'}\right)}{\sum u_i{}^{n'+1}}\right| < \varepsilon_u \qquad (40)$$

Where n' is the number of iterations, i the unknown quantity, and ε_u is the collecting tolerance difference that controls the calculation accuracy. In this paper, ε_u is calculated at 10^{-5}, and the calculation accuracy and time are reasonable.

The boundary conditions were determined by the parameters of two kinds of polymer melt materials and the spinning process, shown in ***Table 2***. [11]

There was no slip flow on the wall surface of the micro hole, and the wall temperature was set as 288 °C; the melt inlet flow is $Q_A = Q_B = 2 \times 10^{-8}$ (m^3/s) (including $Q\,A$ for PA6 inlet flow, $Q\,B$ for PET inlet flow), with a flow ratio of 1:1, (including: $Q\,A$ for PA6 inlet flow, $Q\,B$ for PET inlet flow) and 1.8 mm, at an inlet angle of 75 °C. Calculation results of the velocity field at the entrance and exit of the micropores are shown in ***Figure 5***.

Figure 5 shows that the inlet flow phase into the jet hole happens at the same time, The melt velocity distributions of PET and PA6, two kinds of polymer, are basically the same, which is mainly due to the two different kinds of melt viscosity after the two melt composites, With the PA6 melt viscosity, there is less friction and the speed of the melt is bigger, therefore, there is a maximum speed of the composite melt in PA6 melt at the exit side. The locations of the PA6 axis position, the maximum speed of 0.423 m/s. It is consistent with the conclusion in literature [12-13].

Conclusions

The paper is based on two kinds of polymerisation kinetics and describes a melt control equation established for two concrete symmetrical and complete channels of asymmetric polymer melt flow. For complex melts with symmetric or asymmetric distribution of the velocity field in the tunnel, the above equations are derived for the velocity and temperature field distribution function. Based on polymer material parameters, boundary conditions, the iterative algorithm of the polymer melt velocity and temperature distribution, theoretical guidance on technological parameters and their distribution for the composite profiled fibre forming interface may be extended. The velocity and temperature distribution curve, structural parameters of the composite fibre spinning components, and forming process parameters can be calculated to lay a theoretical basis for design.

Acknowledgements

This work was supported by the China Postdoctoral Science Foundation (item number: 2019M652145) and the National Key Research and Development Program of China (item number: 2016YFB0302900-2016YFB0302901-1). The authors of this paper appreciate each participant in the discussion.

References

1. Tao XM. Study of Fiber-Based WearW able Energy Systems. *J Acc Chem Res*. 2019; 52(2): 307-315.
2. Takeshi KJ, Radhakrishnan, Sadaaki A, Akira T, Norimasa O, Xia Jin, et al. High-Speed Melt Spinning of Bicomponent Fibers: Mechanism of Fiber Structure Development in Poly (Ethylene Terephthalate)/Propylene System. *J Appl Polym*. 1996; 6(11): 1913-1924.
3. Nakajima T. *Advanced Fiber Spinning Technology*. Woodhead: Cambridge; 1994.
4. Boonlertsamut J, Thumsorn S, Umemura T, Hamada H, Sakuma A. Spinnability and Characteristic of Polyoxymethylene-Based Core-Sheath Bicomponent Fibers. *J Eng Fiber Fabr.* 2019; 14:1-7.
5. Tallury SS, Pourdeyhimi B, Pasquinelli MA, Spontak RJ. Physical Microfabrication of Shape-Memory Polymer Systems Via Bicomponent Fiber Spinning. *Macromol Rapid Commun.* 2016; 37: 1837-1843.
6. Ayad E, Cayla A, Rault F,Gonthier A. Effect of Viscosity Ratio of Two Immiscible Polymers on Morphology in Bicomponent Melt Spinning Fibers. *Adv Polym Technol*. 2018; 4(37): 1-8.
7. Rwei SP, Lin YT, Su YY. Study of Self-Crimp Polyester Fibers. *Polym Eng Sci*. 2005; 6 (45): 838-845.
8. Tae HO. Melt Spinning and Drawing Process of PET Side-By-Side Bicomponent Fibers. *J Appl Polym Sci.* 2006; 101: 1362-1367.
9. Kikutani T, Radhakrishnan J, Arikawa S, Takaku A, Okui N, Jin X, et al. High -Speed Melt Spinning of Bicomponent Fibers: Mechanism of Fiber Structure Development in Poly (Ethylene Terephthalate)/Polypropylene System. *J Appl Polym Sci*. 1996; 62(11): 1913-1924.
10. Youhei K, Tomoaki T, Yutaka M, Wataru T, Takeshi K. Structure and Properties of Low-Isotacticity Polypropylene Elastomeric Fibers Prepared by Sheath-Core Bicomponent Spinning: Effect of The Composition of Sheath Layer with Constant High-Isotacticity Polypropylene Content. *J Polym Eng*. 2014; 70(3): 203-212.
11. Radharishhnan J, Kikutani T, Okui N. High-Speed Melt Spinning of Sheath-Core Bicomponent Polyester Fibers: High and Low Molecular Weight Poly (Ethylene Terephthalate) Systems. *Text Res J*. 1997; 67(9): 684-694.
12. Han CD, Shetty R. Studies on Multilayer Film Coextrusion I. The Rheology of Flat Film Coextrusion. *Polym Eng Sci* 1976; 16(10): 697-705.
13. Han CD, Shetty R. Studies on Multilayer Film Coextrusion. II. Interfacial Instability in Flat Film Coextrusion. *Polym Eng Sci*. 1978; 18(3): 180-186.

Received 07.12.2020 Reviewed 26.02.2021